Characterization of Laptop Fires in Spacecraft

Rosa E. Padilla [*], Daniel L. Dietrich [†], Gary A. Ruff [‡], and David L. Urban [§]

NASA John H. Glenn Research Center, Cleveland, Ohio, 44135, USA

Kelly C. Lynch [¶]

University of Kentucky, Chemical Engineering Department, Lexington, Kentucky, 40506, USA

Alfredo Juarez[‖], Susana A. Harper [**]

White Sands Test Facility, Las Cruces, New Mexico, 88012, USA

and

Christopher R. Nagel [††]

NASA Johnson Space Center, Houston, Texas, 77058, USA

An accidental fire involving the Lithium-Ion (Li-ion) battery in a laptop computer is one of the most likely fire scenarios on-board a spacecraft. These fires can occur from a defect in the battery that worsens with time, over-charging the battery and leading to failure or accidental damage caused by thermal runaway. While this is a relatively likely fire scenario, very little is known about the how a laptop computer fire would impact a sealed spacecraft. The heat release would likely cause a pressure rise, possibly exceeding the pressure limit of the vehicle and causing a relief valve to open. The combustion products from the fire could pose a short-term and long-term health hazard to the crew and the fire itself could cause injury to the crew and damage to the spacecraft. Despite the hazard posed by a laptop fire, there is little quantitative data on the fire size, heat release and toxic product formation. This paper presents the results of initial attempts to quantify the fire resulting from a failed laptop battery tested at the NASA White Sands Test Facility (WSTF). The fire size and characteristics such as maximum heat release rate, total heat release, maximum temperatures and fire duration are determined. Using existing models and correlations for fires, the measured fire characteristics are extrapolated to laptop fires on a vehicle the approximate size of the Orion spacecraft.

Nomenclature

ΔT_c = Centerline temperature, K

ΔT_o = Temperature, K

ρ = Air density, kg/m^3

A_s = Surface area, m

c_p = Specific heat, J/K

D = Fire source diameter, m

[*] Aerospace Engineer, Combustion Physics and Reacting Processes Branch, Mail Stop 110-317L
[†] Aerospace Engineer, Combustion Physics and Reacting Processes Branch, Mail Stop 110-3
[‡] Aerospace Engineer, Exploration Systems Project Office, Mail Stop, 162:321-43
[§] Branch Chief, Combustion Physics and Reacting Processes Branch, Mail Stop 77:101
[¶] Undergrad, University of Kentucky, Chemical Engineering Department, Lexington, KY, 40506, USA
[‖] WSTF Flammability Project and Facility Lead, Materials and Components Laboratories, Mail Stop 800-116
[**] WSTF Standard Testing Project and Facility Manager, Mail Stop 803:100
[††] Project Manager, Life Support Systems Branch (EC3), Orion ECLSS GFE, Mail Stop 7A:225

H_F	=	Flame height, m
Q	=	Heat Release rate, kW
Q_c	=	Convective energy release, kW
T_∞	=	Ambient temperature, K
z	=	Height above the fire surface, m
z_o	=	Virtual origin, m

I.   Introduction

THE demand for lithium-ion (Li-ion) batteries has increased throughout the years due to their attractive energy characteristics. Li-ion batteries are known for their wide range of high energy and power density and have become a preferred energy source for many ground and on orbit applications. Among the batteries available, the traditional 18650 cylindrical cell was originally designed for portable electronics, such as hand held power tools and is now in high demand by the automotive industry. Li-ion batteries are also present aboard current spacecraft; the 18650 cells are found in satellites, powertools, and spacesuits as battery packs, while commercial laptops have either 18650 batteries or pouch cells [1]. The Li-ion polymer pouch cells are typically found inside laptop notebooks and in cellular phones. Li-ion batteries pose a serious safety risk for spacecraft and the crew since they can generate large quantities of heat during a thermal runaway event.

Li-ion batteries can release toxic substances, among those are carbon monoxide (CO), carbon dioxdide (CO_2) and other trace species. These gases can be fatal if inhaled in large quantities, primarily a concern to spacecraft crew as these may be asphyxiant or can cause anoxia [2]. During a thermal runaway event, Li-ion batteries can release the fluorine content of the electrolyte and other materials in the battery, such as the polyvinylidene fluoride (PVdF) binder and phosphoryl fluoride (POF3) from the electrodes.

In addition, other gases may form such as hydrogen fluoride (HF), and hydrogen cyanide (HCN)[2]. The total amount of these toxic gases vary considerably depending on manufacturers, state of charge, battery type and chemistry.

There have been numerous studies of the failure modes and performance characteristics of a cylindrical or pouch battery during a thermal run away event [3]. However, very few have focused on laptop battery fires. Laptop battery failures have happened worldwide due to defects in the interior parts, such as deformities in the cathode metal or damage to the separator [4]. A few accidents involving laptop fires have occurred through out the years, among those Sony, HP and Dell, have recalled of 1.8 million batteries [5] due to being potential hazards caused from metallic defects and unwanted contact between electrodes. Efforts from Meyer et al. [6], Juarez et al. [7] and Harper et al. [8] have focused on studying the spacecraft smoke alarm thresholds and fire suppression effectiveness on laptop fires. The studies examined laptops that the Orion Program identified as the largest stored-energy source that may be found onboard. The laptops identified were the Surface Pro 42 Whr with 4 cells and the Dell Model No. XPS 15 9560 with six cells at 97 Wh.

This paper focuses on characterizing the fire from a commercial Dell XPS laptop and Surface Pro tablet, that was conducted at the NASA White Sands Test Facility [8]. Measurements of flame height were extracted from the combustion process and used to quantify the maximum heat release, total heat release and centerline temperature using Heskestad's equations.

II.   Experimental Description

Figure 1 shows a general schematic of the experimental apparatus used to perform battery fire tests inside a 1.4 m³ (50 ft³) chamber. This work used a Dell 97 Wh laptop that holds a 6 cell battery pack at a nominal 11.4 V and 25.8 Ahr rating and a Surface Pro that has 4 cells with a nominal 15.14 V and a 11.88 Ahr battery pack. Further specifications are found in Table 1. The testing included the laptop unit and the battery pack, which includes electronics and plastic housing. In addition, the Surface Pro was tested with a keyboard attached. The laptops were charged to a state of charge of 100%.
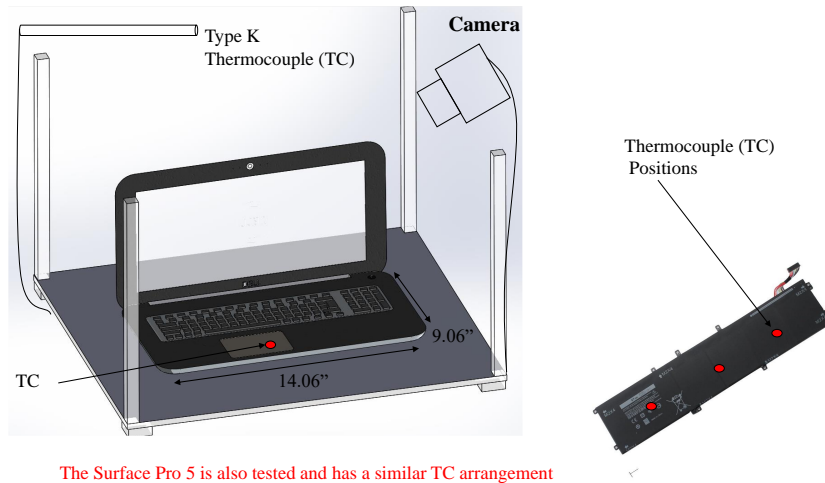
Figure 1: A commercial laptop, Dell XPS 97Wh is forced into thermal runaway inside a 1.4 m^3 (50 ft^3) chamber. A stove top coil element is used to initiate the combustion process. Thermocouples are placed for event monitoring (red dots).

The laptop and tablet were heated externally to promote thermal runaway using a stove top coil element with a power input at approximately a maximum of 1000 W. Two "sparkers" were used to ignite the gases that have been vented out or produced during the pyrolysis process. The chamber and the laptop were instrumented with thermocouples; two Type K thermocouples were reported by Harper et al. [8] as being placed at 0.61 m (24 in.) and 0.864 m (34 in.) above the laptop to monitor potential worst-case cabin temperature conditions during a fire event. The temperature in the chamber stayed between 300-337.45 K. Each individual pouch cell had a thermocouple attached for temperature data upon ignition and propagation. An additional thermocouple was placed above the external casing and above the heater element to verify adequate heat input.

A video camera was placed inside the testing chamber and captured the burning process for all combustion events (as shown in Fig. 2). The flame height was determined from a customized Matlab code developed for image processing of the digital still frames. Pixel data was obtained from the images and converted into real dimensions; the scale factor used was found by measuring the depth from one side of a laptop and divided by the number of pixels. Typical images used for the analysis are seen in Fig. 2. The still images are converted to grayscale by eliminating the hue and saturation information while retaining the luminance. The grayscale images are converted to binary by replacing all pixels in the color image with luminance greater than the threshold level with 1 (white) and replacing all other pixels with the value 0 (black). Figure 2 illustrates the flame height as H$_f$ and D as the diameter of the fire.
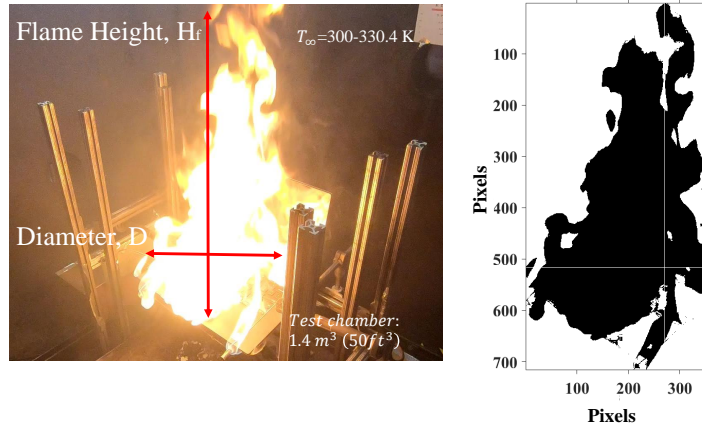
Figure 2: Typical images capturing the burning process, test chamber volume, and ambient temperature. A black and white image used for the analysis of heat release is also shown.

Fire suppression was accomplished with a portable fire extinguisher (PFE) assembly that holds 6 pounds of water and 1.2 lb of nitrogen pressurized to approximately 1270 psia. Details on the portable fire extinguisher are further discussed in Rodriguez et al. [9] work. In addition, the work by Harper et al. [8] discusses the use of the PFE on a Dell XPS 15 fire and its capability of extinguishing a Dell XPS 15 with 2 lbs of water. The chamber was instrumented with an Orion smoke detector, particulate sensor, and gas probes to perform toxicological analysis of CO, CO_2 and O_2, among other hydrocarbons.

III.   Results

I   Burning Behavior

Figures 3, 4, and 5 show the combustion process of a fully charged Dell XPS 97 Wh laptop. Images from the burning process for the Surface Pro are not shown in this paper. The burning of a laptop can be summarized into the following stages: the heater is turned on and the laptop is heated for about 180 s, raising its temperature to pyrolize the laptop or battery and cause a release of gaseous products. The laptop begins to decompose and shows a minimum amount of white smoke (see Fig. 3a) and sparks under the mousepad and sides. The sparks resemble what has been previously reported in literature to occur when solid electrolyte burns as its being ejected. These gases are ignited using a sparker and the coil was shut off when the laptop was uniformly ignited over the exposed area. The Li-ion battery pack is found under the mousepad region; the mousepad is shown to raise during the heating period which is an indication that pouch cells go through a minimum amount of swelling. The second phase shows a large amount of white smoke (see Fig. 3b) and more apparent sparks are released from the sides and underneath the mousepad. The venting period lasted for about 6 s. The released smoke is ignited and results in an aggressive fireball ("thermal"[10]) outburst 2 seconds after the end of the venting period (Fig. 4a). The white smoke is also observed midway during the fire suppression phase (Fig. 5a).

4

(a) The heater is turned on and a small quantity of white smoke begins to appear.


(b) White smoke and sparks are released through the mousepad and from the sides of the laptop.

Figure 3: Digital still images displaying the initial combustion event from a 97Wh Dell laptop.

The fire begins to reduce in its hemispherical shape and instead elongates (Fig. 4c), showing three regions, a continuous, intermittent, and buoyant plume, as described by McCaffrey [11]. The flame rapidly moves to the sides, pulses and flickers. The flame abates and reduces in size significantly while spreading above the region where the battery pack is located (near the mouse pad area) and is shown in Fig. 4d. A second outburst occurs 4 seconds after introducing water, as shown in Fig. 4e. After introducing water, the fire grows in size briefly and then begins to cool. Very near extinguishment the fire is pushed to other areas in the laptop, as shown in Fig. 5a. A typical post image after the fire event is shown in Fig. 5b. The image was taken from Harper et al. [8] work. The image shows the thermal runaway propagation which occurs across all cells when external heating was applied directly underneath the coil heater. A visual observation of the cells after combustion shows the exterior packaging foil of the battery pack and the pouch cells completely burnt. Molten case material was also emitted in the Dell more than what was observed in the Surface Pro. In addition, the smoke may be due to the decomposition of the plastic case and a contribution from the pouch cell material (i.e. separator melts). Similar heating behavior was observed with the Surface Pro, however, the fire was not suppressed and lasted for 8 minutes of continuous burning. A large amount of white smoke and a large fire size was also observed.

(a) The first flame outburst.
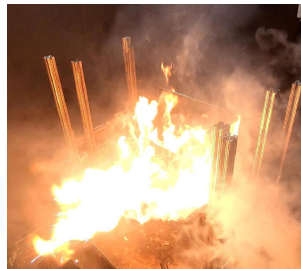
(b) The flame moves to the sides.

(c) An elongated plume appears.

(d) Fire sits above mousepad area.

(e) Second fire outburst.

(f) Flame abatement.

Figure 4: Digital still images displaying the combustion process of a 97Wh Dell XPS laptop at different time stamps.

(a) Near extinguishment.

(b) Thermal runaway propagation to all battery cells.

Figure 5: Digital still images displaying the combustion process of a 97Wh Dell XPS laptop showing post images of the battery pack.

Figure 6a shows the evolution of the thermal runaway event in the Dell XPS 15 and the temperature profile for the Surface Pro 5 is shown in Fig. 6b. The three stages that can observed in the plot are summarized in Fig. 6 as follow: a linear rise in temperature until about 318 s to 415 K due to the initial heating applied by the coil. The temperature increases upon heating until it reaches the melting temperature of the laptop casing. In addition, the temperature jump may also be associated to the venting and decomposition period in a pouch cell. The melting temperature of a typical pouch cell separator from either polyethylene or polypropylene is reported in literature to be between 403.15-438.15 K [12] which is close to the first temperature jump. The second temperature jump is a typical thermal runaway behavior that has also been captured in Li-ion 18650 battery studies. The thermal runaway onset temperature is between 513.4-600 K (shown as dashed ellipses in Fig. 6), which is higher than what is observed in 18650 and pouch cells. The thermal runaway event happens within a few seconds (6-36 s) and experiences a sharp temperature rise from 513.4 K to 943.4 K (T_{max}) for the Dell XPS laptop and from 600 K to 800 K in 36 s for the Surface Pro. The average runaway power during this period can be estimated from the total energy released (discussed in Section III) that is at 326.2 kJ for the Dell XPS this can produce about 54.3 kW within 6 s. The cooling stage occurs right after the T_{max} peak temperature, showing that cooling occurs at a faster rate for the Dell XPS than the Surface Pro.
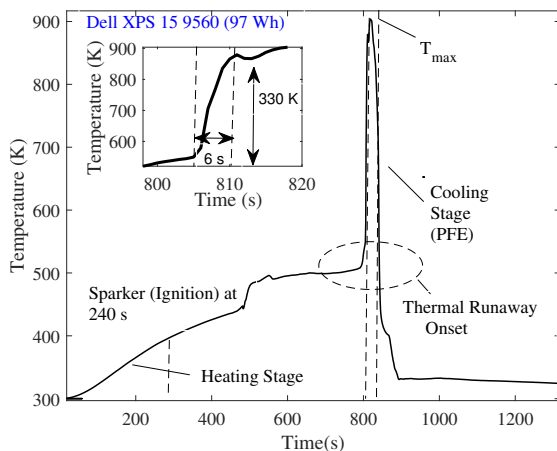
(a) Temperature as a function of time for the Dell XPS.
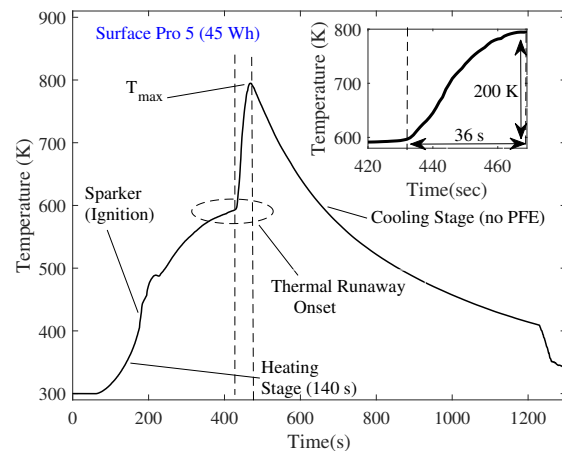
(b) Temperature as a function of time for the Surface Pro.

Figure 6: Temperature profiles showing the combustion event for the Dell XPS and the Surface Pro. The inset image zooms into the thermal runaway region.

II   Flame Height

Figures 7, 8 and Fig. 9 show the flame height and diameter as functions of time for the Dell XPS and Surface Pro. In general, the flame size for the Dell decreased with time, but exhibited large fluctuations or flare ups. The flame reaches a height of 0.85 m (t=281.1 s) during the first outburst, 0.9 m (t=288.1 s), and 0.63 m (t=296.7 s). The flame height then decreases linearly to as low as 0.3 m (t=299-313 s). Figure 7 also shows locations where the water

suppression became active (t= 315-327 s). A fourth outburst was observed during the fire suppression and caused the flame to reach a maximum of 0.65 m (319.2 s) as shown by the secondary outburst peak, in Fig. 7. Figure 8 shows that the Surface Pro remained at a lower height than the Dell XPS 15. The fire size reached a height above 0.8 m, and rapidly decreased to 0.6 m while remaining at about 0.15 m during abatement. Water was not used to extinguish the fire during the period that the combustion event was observed. Flame height measurements during the first outburst are obscured by the amount of white smoke released during the event by ±2 in (0.05 m). In general, image processing code can be tuned to capture the highest fire intensity region, while leaving out areas that are not of interest.
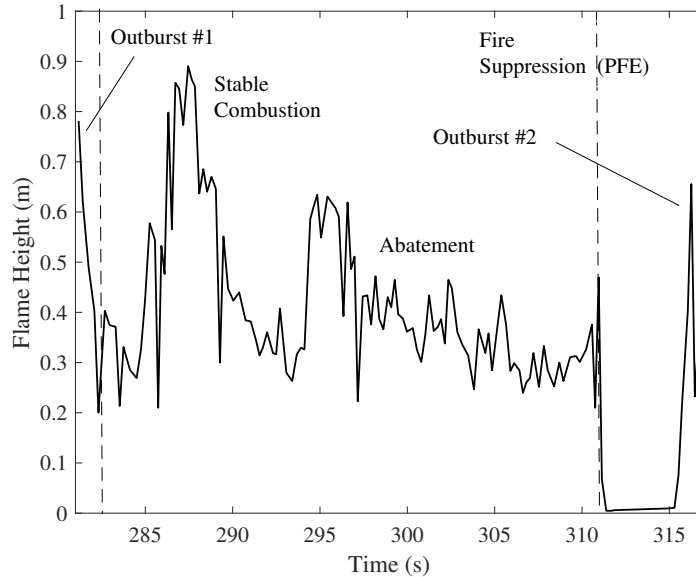

Figure 7: Measured flame height for the Dell XPS as a function of time divided into various stages to describe the burning phenomena. Flame height reached between 0.85 and 0.6 m, respectively.
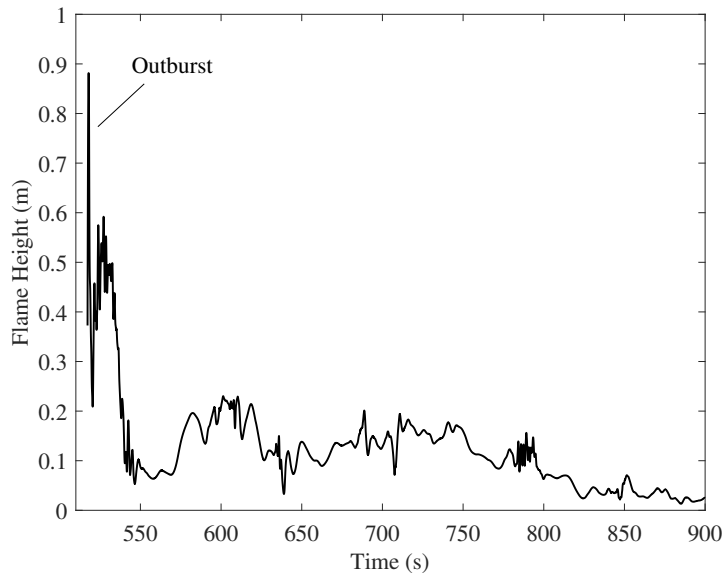

Figure 8: Measured flame height as a function of time for the Surface Pro 5.

7

The flame width is measured by analyzing the extracted images from the video. Figure 9 shows the flame diameter reached over 0.9 m during the first outburst (Fig. 4a) and thereafter it varies between 0.2-0.65 m. The second outburst had a diameter of 0.7 m. The outburst are described in Dinenno et al., as a thermal or "fireball" [2, 10], which occur from a sudden release of a finite volume of gaseous fuel that is ignited. Flame width for the Surface Pro is not shown in the paper. However, the Surface Pro showed a similar behavior, that is, a maximum diameter reached above 0.8 m and thereafter remained between 0.6 and decaying down to 0.2 m. The diameter of the Surface Pro was obscured since the fire propagated to different locations along the surface of the tablet.
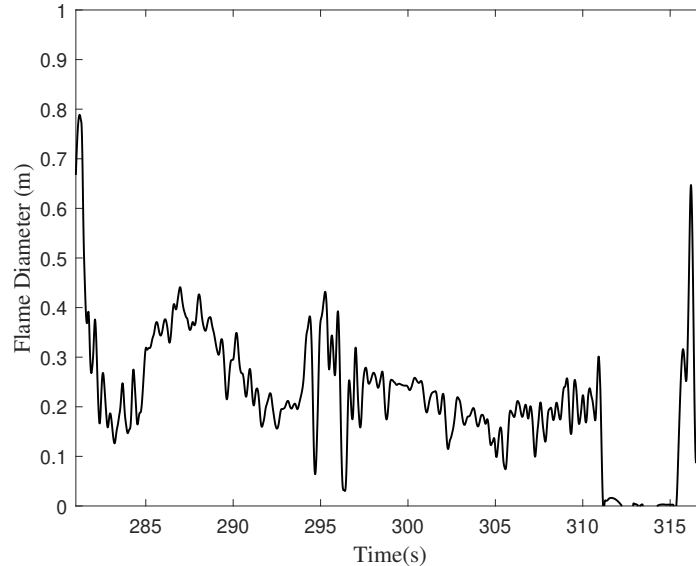

Figure 9: Flame diameter for the Dell XPS 15.

III Heat Release

The heat release rate (HRR) is among the most important parameters for understanding combustion processes. The heat release rate gives insight on the fire size, rate of smoke production, and overall an evaluation for fire assessment in a new environment [2]. In the event of an accidental fire inside a spacecraft vehicle, the heat release will cause a temperature rise in the cabin. The primary mechanism to dissipate the heat from the cabin gas is radiation and convection heat transfer to the vehicle and through the ECLSS systems [13]. Preliminary measurements of heat release have been made in this paper using the WSTF data [8] as an effort to understand the impact that a fire would have inside a spacecraft vehicle. In addition, very little data is available on heat release measurements made on laptops units. The cone calorimeter is most commonly used worldwide for measuring heat release for many materials and are described in ASTM E1354 and ISO 5660 [14]. This work has measured heat release from a Dell 97 Wh laptop and Surface Pro 5 42 Wh fire using measurements of flame height. The Heskestad [15] correlation was used to calculate the energy release rate, $\dot{Q}$ (kW) and is typically used to characterize liquid pool fires with a defined fire source diameter, D (m) and flame height, H_F(m),

$$H_f = 0.235\dot{Q}^{2/5} - 1.02D \tag{1}$$

The heat release is based on flame height measurements and on the diameter of the flame. Figure 10 and 11 shows the measured heat release profiles as a function of time.Figure 10 shows the first maximum HRR peak is observed during the first outburst (Fig. 4a) event, rising quickly up to 110 kW (t=281 s) and rapidly decaying thereafter; the fist heat release outburst occurs at a temperature of 900 K based on the surface temperature measured on each cell (Fig. 6). The initial outburst includes more heat that has been released from heating the laptop unit and battery material that was abruptly released from the laptop unit. A second heat release peak is observed at 75 kW (t=286.9 s), and following that at 46 kW (t=294.8 s) peak during stable combustion abatement. However, at t=310 s and between 315-329 s, there is cooling that occurs from the discharge of the fire extinguisher. A maximum outburst of 50 kW in heat release is

International Conference on Environmental Systems

observed after introducing the water. The heat release profile for the Surface 5 Pro is shown in Fig. 11. A maximum heat release rate value is observed above 80 kW during the first outburst and rapidly decays to 50 kW. In general the heat release depletes thereafter. During the major heat release outbursts, preliminary measurements on toxic gases have been observed, such as, HCL (max 30ppm), CO (max 350 ppm), CO_2 (0.5% vol), and HCN (max 2.2 ppm) have been measured. A lack of data has been found for commercial laptops, however, the work by Larsson et al. [16, 17] has performed a study with two Lenovo laptop battery packs, each at a nominal capacity of 16.8 Ah (each battery pack with 6 cells); the heat release measured was between 35-57 kW. The battery packs included the electrical connectors, plastic housing and the electronic circuits, but did not include the laptop casing. However, assuming that the laptop is made from PolyMethylMethAcrylate, the work from Biteau et al. [18] has measured a maximum of 8 kW in heat release using various calorimetry methods. A typical heat release value for a 2.9 Ah (11 Wh) pouch cell was measured by Ribiere et. el. [19] to be 20 kW (at 100% state of charge). The heat release measurements were done with an oxygen consumption method, which based on Ribiere et al. [19] estimates an uncertainty of 10%. Additional work from Hasegawa et al. [20] has measured heat release of a pallet of laptops which included their packaging. The results by Dietrich et al. [13] showed that fires between 50 and 100 kW are detrimental and can cause severe damage to a person tracheal or cause skin burns.
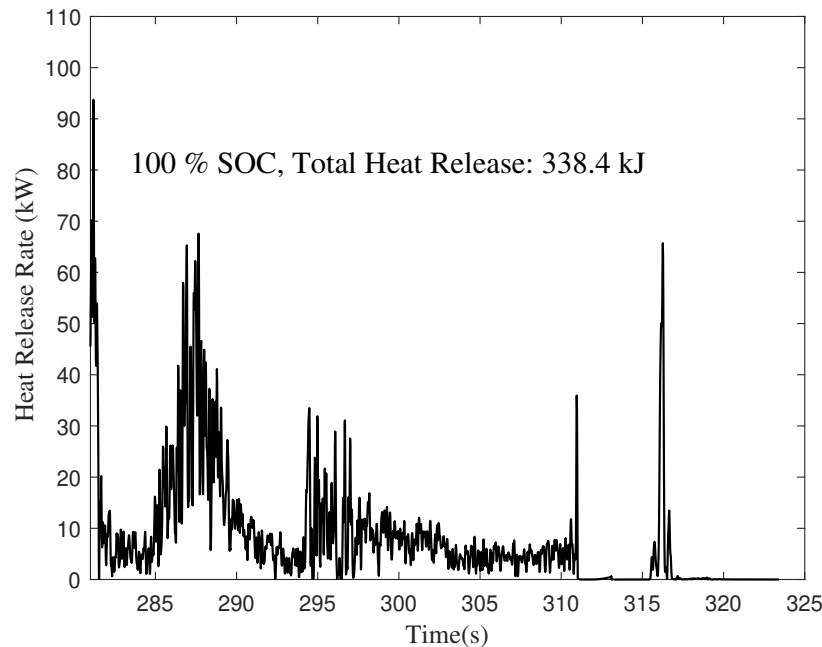

Figure 10: Heat release rate and total heat release are measured using Heskestad et al. [15] correlation for the Dell laptop.
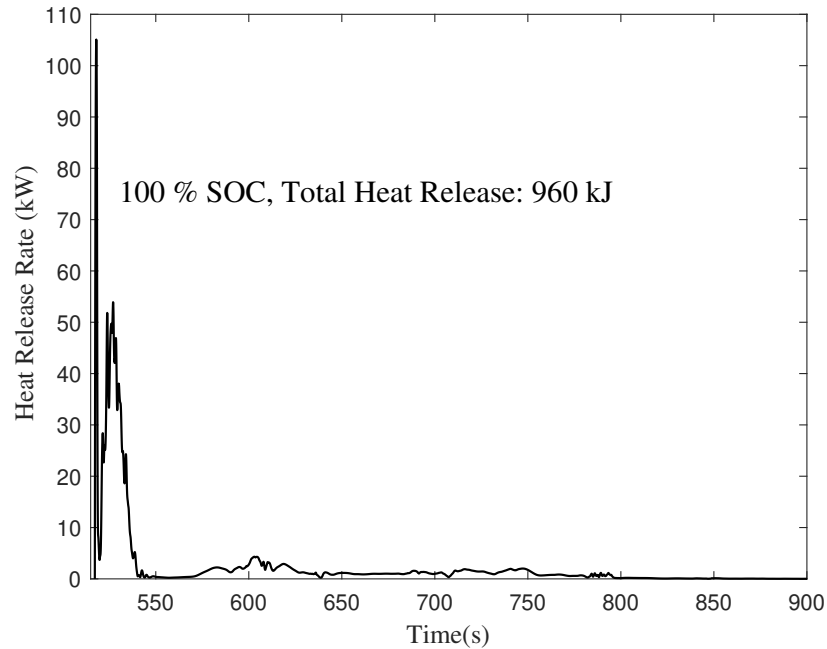
Figure 11: Heat release rate and total heat release are measured using Heskestad et al. [15] correlation for the Surface Pro tablet.

Figure 12 summarizes typical flames with corresponding measured flame height versus heat release. The flame height is closely associated with the amount of energy being released by a fire ($\dot{Q}$). The deviation of the flame height measurement grows with increasing heat release because the larger flames flicker more, yielding and increase in frame-to-frame variation in the flame (shown as Fig. 4c). A difference in $\pm$ 30 kW was observed for fires with longer plumes and less with steadier fires $\pm$ 10 kW (shown in Fig. 4d). In addition, a high uncertainty in height and diameter resulted with the first and second major outbursts (Fig. 4a) and in the presence of high vapors (white smoke) release.
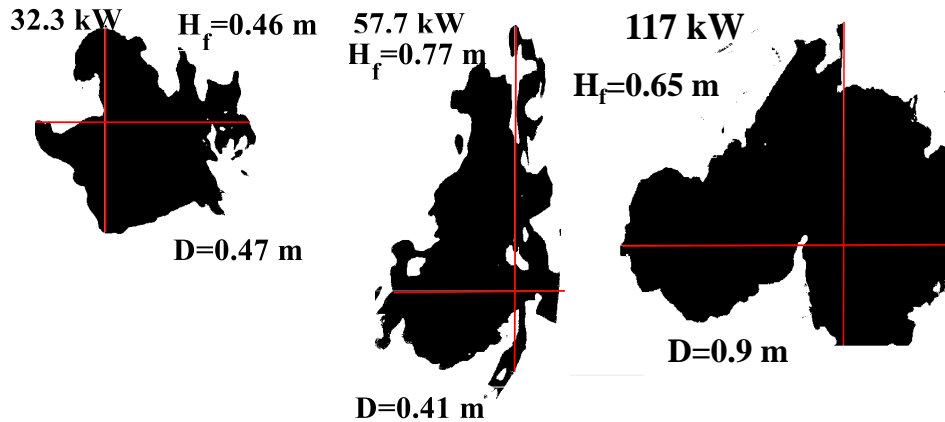
Figure 12: Major combustion events are selected with corresponding heights and maximum heat release values.

The calculated total heat release was measured by integrating the heat release profiles, in Fig. 10 and 11 for the Dell XPS laptop and the Surface Pro. The total heat release from the laptop was measured to be 338.2 kJ and 960 kJ for the tablet, showing that the Surface Pro had a higher heat release due to a higher amount of material getting consumed and no water being introduced. Further work using various calorimetry measurements will be done to quantify and validate the total heat release measured in this preliminary study. As described in the experimental section, the Dell 97 Wh laptop holds a 6 cell battery pack with a nominal 11.4 V and 8.5 Ahr rating. This gives a maximum stored energy of 350 kJ. The Surface Pro has 4 cells with a total of 15.14 V for a 11.8 Ahr rating. This gives a maximum

International Conference on Environmental Systems

stored energy of 647.5 kJ. Additional details are given in Table 1 and shows that the specific energy for the Surface pro is higher than the Dell XPS. The total heat release for the Surface Pro indicates that more of the material was consumed than with the Dell XPS. However, the Dell XPS was suppressed with water, which may be responsible for the lower heat release. Larsson et al. [16, 17] performed a study with two Lenovo laptop battery packs, each at a nominal capacity of 16.8 Ah (each battery pack with 6 cells). The battery packs included the electrical connectors, plastic housing and the electronic circuits, but did not include the laptop casing. The total heat release measured was 3,470 kJ (i.e. 1,735 kJ for one battery pack). In addition, the work from Ribiere et al. [19] and Walters et al. have found that total heat release and maximum peak release are independent of state of charge. That is, at higher state of charges, Ribiere et al. [19] measured a lower total heat release than at a lower state of charge. These preliminary heat release findings surpass the limits that a spacecraft and crew are able to tolerate.

Characteristics	Values	
	Surface Pro 6 (Calculated)	Dell XPS 15
Manufacturer	Microsoft	Dell
Number of Cells	2S2P	3S2P
Dimensions (mm)	292 x 201 x 8.5	13 x 235 x 357
Nominal Voltage (V)	15.14	11.4
Discharge Capacity (Ah)	11.88	8.5
Discharge Energy (Wh)	179.86	97
Mass (kg)	0.77, 0.2-0.3 (estimate battery pack)	1.8 ,0.34 (battery pack)
Battery Pack Dimension (mm)	254 x 101.6 x 3	71.80 x 330.5 x 7.20
Stored Energy (kJ)	647.5	350
Specific Energy (Wh/kg)	900-600	285.3

Table 1: Specifications of the Dell XPS 15 9560 and Surface Pro Tablet. The chemistry of the pouch cell has not been reported by the manufacturer.

Predicted temperatures along the plume's centerline axis are shown in Fig. 13 and are computed using Heskestad's [21] Eq. (2), which depends on the convective energy release, $\dot{Q}_c$ (kW) (Q_c=0.7 $\dot{Q}$) and the temperature of the ambient gas, T_∞. The highest temperature observed inside the testing enclosure was T_∞= 330 K.

$$\Delta T_o = 9.1 \left(\frac{T_\infty}{g c_p^2 \rho_\infty^2} \right)^{1/3} \dot{Q}_c^{2/3} (z - z_o)^{-5/3} \tag{2}$$

where z (m) is the height above the fire surface, total heat release rate $\dot{Q}$ (kW). The virtual origin z_o= 0.083 $\dot{Q}^{2/5}$-1.02 D (m) [21], depends on the diameter of the fire source. Properties of ambient air (density, ρ (kg/m^3) and specific heat, c_p (kJ/kg K) are also included. Figure 13 shows the centerline temperature evaluated for fires between 50 kW-110 kW (assuming complete combustion of the laptop unit) with a maximum fire source diameter of 0.48 m (i.e for non-circular objects, $D = \sqrt{(4A_s)/\pi}$ and A_s is the surface area of the laptop), which corresponds to the diameter of the Dell XPS. .
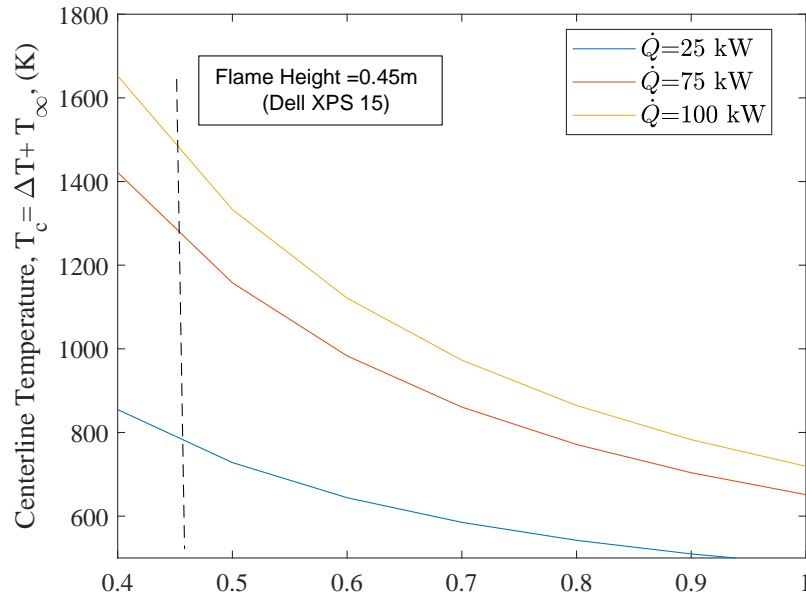
Figure 13: Predicted temperature on the plume's centerline for 25, 75 and 100 kW fires with a diameter of D=0.48 m.

The centerline temperature for a 25, 75 and 100 kW fire at a height of 0.45 m results in plume temperatures above 1550, 1380 K and 800 K, respectively. Future work will investigate and measure flame temperatures with pyrometry methods.

IV. Conclusion

Experimental data from a test conducted at WSTF was used as an initial effort to characterize the fire behavior in commercial laptops (DELL XPS 15 at 95 Wh and the Surface Pro 42 Wh). The test was conducted inside of a 1.4 m^3 (50 ft^3) chamber to contain combustion by-products. Digital still frames were extracted and were used for measurements of height and heat release. The height measurements were then used to calculate the maximum heat release using Heskestad correlations, total heat release, and the centerline flame temperature.

A coil stove top at 1.0 kW was used to initiate thermal runaway. During the first stage of the burning process, the laptops and tablets were seen to release a drastic amount of white smoke for about 6 s due to material decomposition. The venting period followed an aggressive flame outburst. The Surface Pro was burnt continuously for 8 min, while the Dell XPS was burning for 70 s and thereafter water suppression was introduced. The Dell XPS experienced a second outburst 3 s after the suppression event. The temperature profile showed the dramatic thermal runaway event during a short window span, that is between 6-36 s, while reaching a maximum temperature of 900 K. The temperature profile also revealed thermal onset temperatures, between 513.4-600 K, higher than typically observed in the thermal runaway processes for 18650 or pouch li-ion cells.

Using experimental measurements of flame heights the heat release rate and total heat release was approximated with the Heskestad correlations for the two commercial laptops. A heat release between 50-110 kW was observed during the burning process of the laptop and tablet. The flame heights varied between 0.85-0.2 m, while increasing with an increase in heat release. In addition, the flame diameter varied between 0.4 m-1.0 m, decreasing with an increase in heat release. The total energy release associated with the combustion was computed based on experimental measurements of flame height and found to be 338.4 kJ for the Dell XPS and 960 kJ for the Surface Pro tablet. Centerline temperatures between 1550-800 K were predicted using Heskestad's correlation for fire sizes between 25-100 kW and a flame height of 0.45 m. Future work will focus on alternative ignition methods and calorimetry methods in order to validate the data that was presented in this paper.

Acknowledgments

the experiments.

References

[1] McKissock, B., Loyselle, P., and Vogel, E., "Guidelines on Lithium-ion Battery use in Space Applications," 2009.

[2] DiNenno, P. J., *SFPE Handbook of Fire Protection Engineering*, SFPE, 2008.

[3] Park, S.-Y., Kim, D.-H., and Im, H.-S., "The Experimental Study for the Combustion-Property of Sandwich Panels using ISO 5660 Cone Calorimeter," *Fire Science and Engineering*, Vol. 20, No. 4, 2006, pp. 33–41.

[4] Spotnitz, R. and Franklin, J., "Abuse Behavior of High-power, Lithium-ion Cells," *Journal of Power Sources*, Vol. 113, No. 1, 2003, pp. 81–100.

[5] "US Consumer Products Safety Commission, HP Expands Recall of Notebook Computer Batteries Due to Fire Hazard,Release 10-240, May 21, 2010," .

[6] Meyer, E., "Spacecraft Fire Safety Research: Combustion of Lithium-ion Batteries to Predict Fire Scenarios," 2018.

[7] Juarez, A., Harper, S. A., Hirsch, D. B., and Carriere, T., "Development of a Standard Test Scenario to Evaluate the Effectiveness of Portable Fire Extinguishers on Lithium-ion Battery Fires," 2013.

[8] Harper, S., Juarez, A., Woods, B., Beeson, H., Coan-Skow, M. R., Nagel, C., Casper, S., and Tarver, S., "Orion Portable Fire Extinguisher Performance Testing against a Laptop Lithion-Ion Battery Stored Energy Fire-Method, Magnesium Fires, & Combustion By-product Toxicity," 48th International Conference on Environmental Systems, 2018.

[9] Rodriguez, B. R., "Development of the International Space Station (ISS) Fine Water Mist (FWM) Portable Fire Extinguisher," *43rd International Conference on Environmental Systems*, 2013, p. 3413.

[10] Quintiere, J., *Fundamentals of Fire Phenomena*, Wiley, 2006.

[11] McCaffrey, B., *The SFPE Handbook of Fire Protection Engineering*, Society of Fire Protection Engineers and National Fire Protection Association, 1995.

[12] Roth, E., Doughty, D., and Franklin, J., "DSC Investigation of Exothermic Reactions Occurring at Elevated Temperatures in Lithium-ion Anodes Containing PVDF-based Binders," *Journal of Power Sources*, Vol. 134, No. 2, 2004, pp. 222–234.

[13] Dietrich, D. L., Niehaus, J., Ruff, G. A., Urban, D. L., Easton, J., and Takahashi, F., "Determination of Realistic Fire Scenarios in Spacecraft," *43rd International Conference on Environmental Systems*, 2013, p. 3411.

[14] ISO, "Fire Tests Reaction to Fire Part 1: Rate of Heat Release from Building Products (Cone Calorimeter Method)," *ISO 5660-1: 1993 (E)*.

[15] Heskestad, G., "Fire Plumes, Flame Height, and Air Entertainment," *SFPE Handbook of Fire Protection Engineering*, Springer, 2016, pp. 396–428.

[16] Larsson, F., Andersson, P., Blomqvist, P., and Mellander, B.-E., "Toxic Fluoride Gas Emissions from Lithium-ion Battery Fires," *Scientific reports*, Vol. 7, No. 1, 2017, pp. 10018.

[17] Larsson, F., Andersson, P., Blomqvist, P., Lorén, A., and Mellander, B.-E., "Characteristics of Lithium-Ion Batteries During Fire Tests," *Journal of Power Sources*, Vol. 271, 2014, pp. 414–420.

[18] Biteau, H., Steinhaus, T., Simeoni, A., Schemel, C., Marlair, G., Bal, N., and Torero, J. L., "Calculation methods for the heat release rate of materials of unknown composition," 2008.

[19] Ribière, P., Grugeon, S., Morcrette, M., Boyanov, S., Laruelle, S., and Marlair, G., "Investigation on the Fire-Induced Hazards of Li-ion Battery Cells by Fire Calorimetry," *Energy & Environmental Science*, Vol. 5, No. 1, 2012, pp. 5271–5280.

[20] Hasegawa, H. K., Alvares, N. J., and White, J. A., "Fire Tests of Packaged and Palletized Computer Products," *Fire technology*, Vol. 35, No. 4, 1999, pp. 291–307.

[21] Karlsson, B. and Quintiere, J., *Enclosure Fire Dynamics*, CRC press, 1999.